Ultrahigh secondary electron emission of carbon nanotubes

Cite as: Appl. Phys. Lett. **96**, 213113 (2010); https://doi.org/10.1063/1.3442491
Submitted: 31 March 2010 . Accepted: 03 May 2010 . Published Online: 27 May 2010

Jun Luo, Jamie H. Warner, Chaoqun Feng, Yagang Yao, Zhong Jin, Huiliang Wang, Caofeng Pan, Sheng Wang, Leijing Yang, Yan Li, Jin Zhang, Andrew A. R. Watt, Lian-mao Peng, Jing Zhu, and G. Andrew D. Briggs

Ultrahigh secondary electron emission of carbon nanotubes

Jun Luo,[1,a)] Jamie H. Warner,[1] Chaoqun Feng,[2] Yagang Yao,[2] Zhong Jin,[2] Huiliang Wang,[1] Caofeng Pan,[3] Sheng Wang,[2] Leijing Yang,[2] Yan Li,[2] Jin Zhang,[2] Andrew A. R. Watt,[1] Lian-mao Peng,[2] Jing Zhu,[3] and G. Andrew D. Briggs[1]

[1]*Department of Materials, University of Oxford, Parks Road, Oxford, Oxfordshire OX1 3PH, United Kingdom*

[2]*Department of Electronics, Key Laboratory for the Physics and Chemistry of Nanodevices, College of Chemistry and Molecular Engineering, Peking University, Beijing 100871, People's Republic of China*

[3]*Department of Materials Science and Engineering, Beijing National Center for Electron Microscopy, The State Key Laboratory of New Ceramics and Fine Processing, Laboratory of Advanced Materials, Tsinghua University, Beijing 100084, People's Republic of China*

(Received 31 March 2010; accepted 3 May 2010; published online 27 May 2010)

The secondary electron emission of the tube bodies of single-walled carbon nanotubes is found to be ultrahigh and comparable with that of diamond, when the nanotubes are connected with electron reservoir. Both of semiconducting and metallic nanotubes possess this property. © *2010 American Institute of Physics*. [doi:10.1063/1.3442491]

When a particle beam, such as an electron beam (e-beam), hits matter, some internal electrons of the atoms are ejected and emitted as secondary electrons (SEs). This is significant for fundamental research, and has applications ranging from electron multipliers for detecting ions and photons[1–5] to crossed-field devices used in microwave ovens and radars,[4,5] where materials with strong SE emission are desired. Materials in current commercial electron multipliers typically have SE yields ranging from 1 to 4.[2,3] The SE yield of diamond is ultrahigh, from 12 to 113.[1,3,4,6,7] Diamond is excellent but expensive. It has been reported that the tips of single-walled carbon nanotubes (CNTs) under e-beam irradiation in a scanning electron microscope (SEM) generate strong SE emissions.[8,9] This is important for CNTs and their potential applications, since mass production of single-walled CNTs is achievable.[10,11] But, the tip is only a small part of a CNT, and the main tube body has perfect atomic and electronic structures that are dramatically different from the tip.[8]

Here we show that the SE yield of the tube bodies of CNTs is up to 123 and comparable with that of diamond, when the CNTs are connected with electron reservoir. We demonstrate that this ultrahigh SE yield is irrespective of whether the CNT is semiconducting or metallic. This not only opens the pathway for incorporating CNTs into applications utilizing SE emission but also has the important implication that the separation of CNTs into their semiconducting and metallic counterparts is not necessary in fields relevant to SE emission.

Our CNTs were fabricated on the oxide surfaces of Si chips by chemical vapor deposition and characterized to be single-walled.[12] The oxide layers were 312 nm thick, much thinner than the thickness of the Si part, 500 μm. The Si part was highly doped and conductive. Figure 1(a) shows a SEM image of some CNTs that exhibited bright contrast. One end of each bright CNT was attached to the conductive Si part that was partially exposed at the chip edge. Figure 1(b) shows the end of CNT No.1 [also indicated in Fig. 1(a)] attached to the Si part, and its other end was located on the oxide surface, as shown in Fig. 1(a). Figure 1(c) presents a schematic illustration of the CNTs with one end attached to the Si part and the other end resting on the oxide surface. After Figs. 1(a) and 1(b) were collected, some of the CNTs

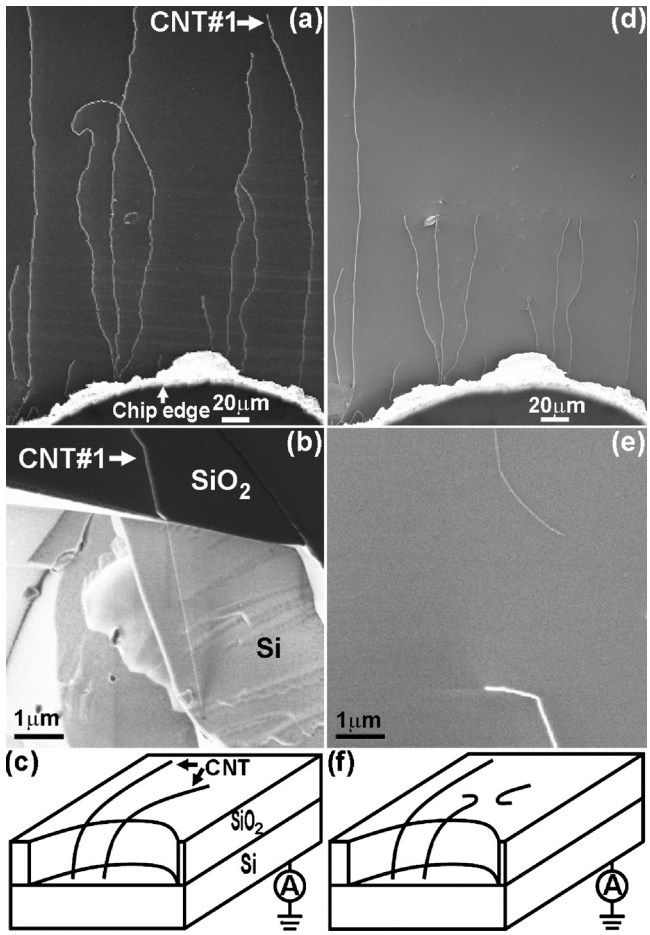

FIG. 1. SEM images of long CNTs lying on the oxide surface of a Si chip. (a) Top view of as-grown CNTs, where the broad bright zone in the lower part is the edge of the chip and the CNTs are roughly perpendicular to the edge. (b) Close-up of an end of CNT NO. 1 located at the chip edge. (c) Schematic illustration (not to scale) for (a) and (b). (d) Top view of the CNTs after some of them were broken. (e) Close-up of the breaking site of CNT No. 1. (f) Schematic illustration (not to scale) for (d) and (e). The Si part of the chip is connected with a current meter.

[a)]Author to whom correspondence should be addressed. Electronic mail: jun.luo@materials.ox.ac.uk.

TABLE I. Data of the SE measurements of the CNTs.

CNT No.	d_{CNT} (nm)[a]	i'' (fA)[b]	i' (fA)	I_b (pA)	L (nm)	δ [c]	Connected with Si[d]	Notes[e]
1	1.48 ± 0.09	0 ± 49	2150 ± 50	-77.75 ± 0.05	2741	41 ± 5	Yes	Before breaking
1	1.48 ± 0.09	-49 ± 49	1450 ± 50	-87.3 ± 0.1	2741	25 ± 3	Yes	After breaking
1	1.48 ± 0.09	-49 ± 49	-49 ± 49	-88.9 ± 0.1	2741	0	No	After breaking
2	2.5 ± 0.3	0 ± 49	1100 ± 100	-60.4 ± 0.1	6042	35 ± 9	Yes	After breaking
2	2.5 ± 0.3	0 ± 49	-25 ± 25	-60.2 ± 0.1	6042	-1 ± 3	No	After breaking
3	2.4 ± 0.2	0 ± 49	1900 ± 100	-53.8 ± 0.2	2741	32 ± 5	Yes	After breaking
3	2.4 ± 0.2	25 ± 74	0 ± 98	-54.1 ± 0.1	2741	-0.4 ± 3.2	No	After breaking
4	1.7 ± 0.1 (1.65)	-49 ± 49	2000 ± 200	-54.1 ± 0.1	2741	49 ± 9 (50 ± 8)	Yes	After breaking; S
4	1.7 ± 0.1 (1.65)	0 ± 98	0 ± 98	-51.9 ± 0.1	2741	0 (0)	No	After breaking; S
5	1.5 ± 0.2	0 ± 98	3000 ± 200	-57.5 ± 0.1	2741	76 ± 18	Yes	After breaking; S
5	1.5 ± 0.2	0 ± 49	-49 ± 49	-56.0 ± 0.1	2741	-1 ± 3	No	After breaking; S
6	2.5 ± 0.2	49 ± 49	953 ± 25	-68.3 ± 0.1	2741	12 ± 2	Yes	After breaking; M
6	2.5 ± 0.2	0 ± 98	-49 ± 49	-68.8 ± 0.1	2741	-1 ± 2	No	After breaking; M
7	1.5 ± 0.2 (0.89)	0 ± 98	3300 ± 200	-66.3 ± 0.1	2741	73 ± 17 (123 ± 12)	Yes	After breaking; M
7	1.5 ± 0.2 (0.89)	0 ± 49	0 ± 98	-67.5 ± 0.1	2741	0 (0)	No	After breaking; M

[a]The values in the parentheses were obtained by RBM and the other values were measured by AFM. The RBM-measured diameter of CNT No. 4 is close to its AFM-measured value but the RBM diameter of CNT No. 7 is rather smaller than its AFM value, possibly because external impurities exist on CNT No. 7.
[b]The zero point of the current meter was 0 ± 98 fA. Thus, all of the measured values of i'' were exactly around zero, indicating no charge in the oxide surfaces (Ref. 14).
[c]The values in the parentheses were calculated with the RBM diameters and the other values were calculated with the AFM diameters.
[d]"Yes" and "No" mean that the corresponding CNT sections are connected and unconnected with the Si parts, respectively.
[e]"S" and "M" denote semiconducting and metallic, respectively.

were scratched by a fine glass tip and broken in half, as shown in Fig. 1(d). Figure 1(e) shows a higher-magnification SEM image of the broken region of CNT No. 1 with the bottom connected section still exhibiting bright contrast, while the top section that is no longer attached to the Si part has reduced contrast. Figures 1(d) and 1(e) illustrate that the unconnected regions of the broken CNTs have significantly less contrast in the SEM images as compared to the connected ones. The long CNT located in the left of Fig. 1(a) is untouched and still retains bright contrast uniformly along its length in Fig. 1(d). Figure 1(f) shows a schematic illustration of the broken CNTs with the bottom section connected to the Si part and the top section unconnected. Since the SEM images were formed by the SE signals emitted by the CNTs, the change in the contrasts of the broken CNTs meant that their SE yields changed. We derive the SE yield δ_{CNT} of a CNT in SEM as[13]

$$\delta_{CNT} = \frac{i'' - i'}{I_b} \times \frac{L}{(1 + \eta_{SiO_2}) d_{CNT}}, \quad (1)$$

where d_{CNT} is the CNT diameter and can be measured by atomic force microscope (AFM) or Raman, and η_{SiO_2} is the backscattered electron yield of SiO_2. I_b is the current of the e-beam of SEM and can be measured by a Faraday cup and the current meter shown in Figs. 1(c) and 1(f). i'' and i' are the leakage currents flowing through the chip to ground when the e-beam is scanning two areas of the same size without and with the measured CNT. They can also be measured by the current meter. L is the size of the scanned area along the scanning direction of the e-beam, while the CNT axis is perpendicular to the scanning direction.

In order to obtain the intrinsic SE yields of CNTs, there should be no charge accumulation on the chip surface induced by the e-beam irradiation, corresponding to the condition that $i''=0$.[14] It was found that when the accelerating voltage of the e-beam was 1 kV and the working distance was 3.6 mm, $i''=0$ for the surface of the chip shown by Fig. 1 (see also Table I). Also, any influence of imaging history was avoided.[13] Under these conditions, the SE yields of CNT No. 1 before and after it broke were measured, and the measurement results are listed in Table I. The value of η_{SiO_2} is between 0 and 1,[15] giving the SE yield of CNT No. 1 before breaking in the range of 26–51. Taking η_{SiO_2} as 0.25 from a renowned database[16] gives the SE yield of CNT No. 1 to be 41 ± 5. After it broke, its connected section showed the SE yield of 25 ± 3. As a comparison, materials in commercially available electron multipliers have SE yields ranging from 1 to 4.[2,3] The SE yields of graphite and amorphous carbon are only 0.81 and 0.543–1.56, respectively, when the accelerating voltage of the e-beam is 1 kV.[16] Diamond has the ultrahigh SE yields of 12–113, of which the range corresponding to 1 kV is 12–43.[1,3,4,6,7] Thus, the SE yield of the main tube body of CNT No. 1 is also among the ultrahigh known values. The SE yields were measured to be 12–123 for the connected sections of other six CNTs, as shown in Table I, and also comparable with that of diamond.

The unconnected sections of the CNTs showed the SE yields around zero. This is because they were not connected with an electron reservoir and so electrons lost in their SE emission processes were unable to be replenished. It is possible that they might attract some of the SEs emitted by the neighboring oxide surface but this amount would be small due to the low SE yield, 1.18, of SiO_2.[16] This limited the ability of these unconnected CNT sections to emit SEs, and the same phenomenon has been reported with diamond.[5] Therefore, it is critical that a conductive pathway to an electron reservoir is established in order to realize the intrinsic ultrahigh SE emission of CNTs.

Further, we find that both of semiconducting and metallic CNTs possess the ultrahigh SE yields, as shown in Table

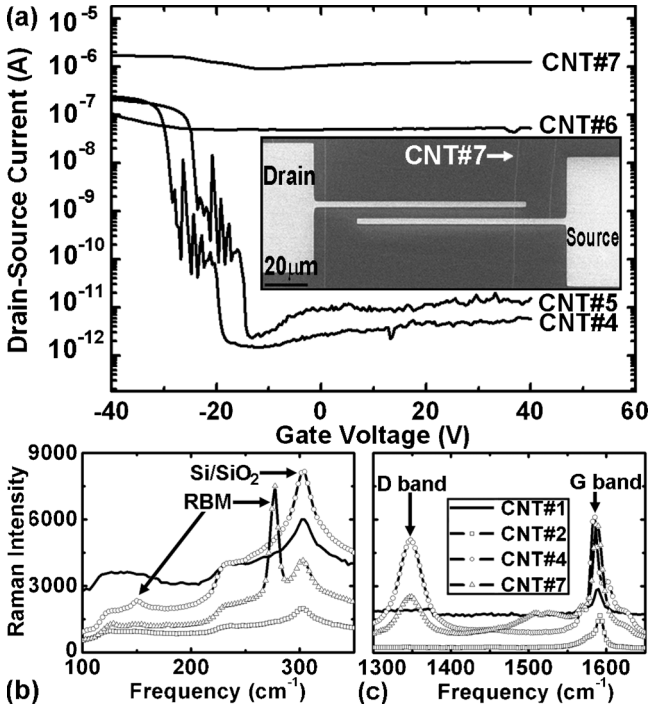

FIG. 2. (a) Dependences of the drain-source currents of CNTs Nos. 4–7 on the gate voltages. The drain-source voltages were fixed at 100 mV during the gate sweeps. The inset is SEM image of the FET of CNT NOs. 7. (b) and (c) Raman spectra of CNTs Nos. 1, 2, 4, and 7 in the frequency ranges of 100–350 cm^{-1} (b) and 1300–1650 cm^{-1} (c).

I. The transport properties of CNTs Nos. 4–7 are shown in Fig. 2(a), showing that the drain-source currents of CNTs Nos. 4 and 5 in their field effect transistors (FETs) can be turned off by the gate voltages and so they are semiconducting. CNTs Nos. 6 and 7 have no gate dependency and are metallic. The inset in Fig. 2(a) shows a SEM image of the FET of CNT No. 7. The SE yields of the four CNTs are in the range of 12–123, when they are connected with an electron reservoir.

The reason why CNTs have ultrahigh SE emissions can be accounted for by the SE emission process.[15,17] After an excited electron in a sample is kicked out of its original site and reaches the sample surface, it needs to overcome the surface barrier to escape into vacuum. It has been calculated that the highest occupied molecular orbital of a CNT is raised above the surface barrier when the CNT is hit by external electrons[8] or carries extra electrons.[18] Thus, the excited electrons in CNTs can get a substantial chance to escape into vacuum.[8,18]

Raman measurement was done on the seven CNTs by using the laser of 532 nm. Due to the match between the laser excitation and the CNT band structures,[19] only CNTs Nos. 1, 2, 4, and 7 showed Raman signals, of which only CNTs Nos. 4 and 7 showed signals of the radial breathing mode (RBM), as shown in Figs. 2(b) and 2(c). The ratios of the intensity of the defect-induced D-band to that of the graphitelike in-plane G-band of CNTs Nos. 1, 2, 4, and 7 are 0, 0, 0.83, and 0.44, respectively. Their SE yields are 25 ± 3, 35 ± 9, 50 ± 8, and 123 ± 12, respectively. Thus, it appears that defects are advantageous to the SE emission. Further investigation is being planned.

The ultrahigh SE emission opens pathway for the application of CNTs as coatings on dynodes of electron multipliers and on cathodes of crossed field devices to improve their device performance.

This work was supported by EPSRC through QIPIRC (Grant No. GR/S82176/01) of U.K., and MOST (Grant Nos. 2006CB932400, 2007CB936202, and 2006CB932701) and NSF (Grant Nos. 50772002 and 20725307) of China. G.A.D.B. thanks EPSRC for Professorial Research Fellowship (Grant No. GR/S15808/01). J.H.W. thanks Glasstone Fund and Brasenose College for support.

[1]G. T. Mearini, I. L. Krainsky, and J. A. Dayton, Jr., Surf. Interface Anal. **21**, 138 (1994).
[2]H. Qin, H. S. Kim, and R. H. Blick, Nanotechnology **19**, 095504 (2008).
[3]G. T. Mearini, I. L. Krainsky, Y. X. Wang, J. A. Dayton, Jr., R. Ramesham, and M. F. Rose, Thin Solid Films **253**, 151 (1994).
[4]G. T. Mearini, I. L. Krainsky, J. A. Dayton, Jr., Y. X. Wang, C. A. Zorman, J. C. Angus, R. W. Hoffman, and D. F. Anderson, Appl. Phys. Lett. **66**, 242 (1995).
[5]A. Shih, J. E. Yater, C. Hor, and R. Abrams, Appl. Surf. Sci. **111**, 251 (1997).
[6]J. E. Yater and A. Shih, J. Appl. Phys. **90**, 3057 (2001).
[7]T. L. Bekker, J. A. Dayton, Jr., A. S. Gilmour, Jr., I. L. Krainsky, M. F. Rose, R. Ramesham, D. File, and G. T. Mearini, Tech. Dig. - Int. Electron Devices Meet. **1992**, 949.
[8]A. Nojeh, B. Shan, K. Cho, and R. F. W. Pease, Phys. Rev. Lett. **96**, 056802 (2006).
[9]W. K. Wong, A. Nojeh, and R. F. W. Pease, Scanning **28**, 219 (2006).
[10]K. L. Jiang, Q. Q. Li, and S. S. Fan, Nature (London) **419**, 801 (2002).
[11]Z. Jin, H. B. Chu, J. Y. Wang, J. X. Hong, W. C. Tan, and Y. Li, Nano Lett. **7**, 2073 (2007).
[12]Y. G. Yao, Q. W. Li, J. Zhang, R. Liu, L. Y. Jiao, Y. T. T. Zhu, and Z. F. Liu, Nature Mater. **6**, 283 (2007).
[13]See supplementary material at http://dx.doi.org/10.1063/1.3442491 for the details of the derivation of Eq. (1) and the SEM operations.
[14]D. C. Joy and C. S. Joy, Microsc. Microanal. **1**, 109 (1995).
[15]K. Kanaya and H. Kawakatsu, J. Phys. D **5**, 1727 (1972).
[16]D. C. Joy, Scanning **17**, 270 (1995); Data available at http://web.utk.edu/~srcutk/htm/interact.htm.
[17]K. Kanaya, S. Ono, and F. Ishigaki, J. Phys. D **11**, 2425 (1978).
[18]J. Luo, L. M. Peng, Z. Q. Xue, and J. L. Wu, Phys. Rev. B **66**, 115415 (2002).
[19]M. S. Dresselhaus, G. Dresselhaus, A. Jorio, A. G. Souza Filho, and R. Saito, Carbon **40**, 2043 (2002).